Usefulness of texture analysis in ^{123}I-FP-CIT for the differentiation of AD and DLB subtypes

Mana Yoshimura[1] MD, PhD,
Elly Arizono[1] MD,
Kei Takase[1] MD,
Mitsuru Okubo[1] MD, PhD,
Yoshitake Takahashi[1] PhD,
Kazuhiro Saito[1] MD, PhD,
Soichiro Shimizu[2] MD, PhD

1. Department of Radiology, Tokyo Medical University, Tokyo, Japan
2. Department of Geriatric Medicine, Tokyo Medical University, Tokyo, Japan

Keywords: ^{123}I-FP-CIT
- Texture analysis
- Gray level histogram moment (GLHM)
- Dementia with Lewy bodies (DLB) - Alzheimer disease (AD)

Corresponding author:
Mana Yoshimura MD, PhD,
6-7-1 Nishishinjuku, Shinjuku-ku,
Tokyo 160-0023, Japan
Tel.: +81-3-3342-6111 (ext. 5818)
Fax: +81-3-3348-6314
radiolmn@tokyo-med.ac.jp

Received:
5 July 2021
Accepted revised:
28 October 2021

Abstract

Objective: I-2β-carbomethoxy-3β-(4-iodophenyl)-N-(3-fluoropropyl) nortropane (^{123}I-FP-CIT) is well known to be a useful tracer for differentiating dementia with Lewy bodies (DLB) and Alzheimer disease (AD). However, clinically, there are some cases in which these diseases cannot be differentiated by ordinary quantitative methods. Therefore, in this study, we established an index that reflects not only the total count but also the distribution and heterogeneity of tracer uptake. We investigated whether assessment of the heterogeneous depletion of ^{123}I-FP-CIT is useful for the differentiation of various types of dementia, i.e., probable DLB, possible DLB, and AD, using texture analysis. **Materials and Methods:** A total of 122 patients with either probable DLB (n=35), possible DLB (n=23), AD (n=44), and normal controls (n=20) were analyzed. Summated single photon emission computed tomography (SPECT) images (7 to 10 slices) of the patients, including the bilateral striatum, were analyzed using the gray-level histogram method (GLHM) of texture analysis. Mean, variance, skewness, and kurtosis of GLHM were compared with the specific binding ratio by Livia Tossici-Bolt's method (SBR). **Results:** The sensitivity and specificity for differentiating probable DLB from possible DLB, AD, and normal controls were 97.1% and 77.0%, respectively, for skewness, using a cutoff point of 6.8%, and 97.1% and 81.6%, respectively, for kurtosis, using a cut-off point of 53.4%. The sensitivity and specificity for differentiating probable and possible DLB from AD and normal controls was 65.5% and 98.4%, respectively, for skewness, using a cut-off point of 6.4%, and 79.3% and 93.8%, respectively, for kurtosis, using a cut-off point of 53.4%. **Conclusion:** In the assessment of the efficacy of ^{123}I-FP-CIT to differentiate AD and DLB subtypes, mean, variance, skewness, and kurtosis by GLHM was as useful as the SBR method. Moreover, possible DLB and probable DLB could be differentiated by skewness and kurtosis. Our results demonstrate that texture analysis is more useful than conventional quantitative methods for obtaining valuable information of the brain. Textural features as such may have considerable potential as imaging biomarkers of DLB progression.

Hell J Nucl Med 2021; 24(3): 206-213 *Epub ahead of print: 17 December 2021* *Published online: 28 December 2021*

Introduction

The dopamine transporter molecular imaging technique using I-2β-carbomethoxy-3β-(4-iodophenyl)-N-(3-fluoropropyl) nortropane (^{123}I-FP-CIT) to analyze presynaptic dopaminergic function is frequently used for the assessment of dopaminergic neurodegenerative diseases (dNDD) and for the differentiation of dementia with Lewy bodies (DLB) and Alzheimer disease (AD). This technique is performed not only by visual assessment but also by semi-quantitative analysis, with the 2 being used together to improve diagnostic ability. Livia Tossici-Bolt's method [1] is a semi-quantitative method for the analysis of ^{123}I-FP-CIT, and has been widely used for a long time. It is performed by calculating the specific binding ratio (SBR), which is the ratio of the specific concentration of the tracer in the striatum to the concentration in whole brain tissue, except for the striatum. A cut-off SBR value of approximately 4.5 was identified to efficiently differentiate normal patients from those with diseases, such as Parkinson disease (PD) or Parkinsonian syndrome (PS). There are some other methods for the same purpose. The cerebrospinal fluid (CSF)-mask algorithm has been developed to reduce the effects of low counts of ^{123}I-FP-CIT in the CSF [2]. Receiver operating characteristic (ROC) analyses indicated that a cut-off value of 3.80 may efficiently differentiate PS from non-PS w-hen using the SBR together with the CSF-mask algorithm. This appears to be similar to the 4.58 obtained by Livia Tossici-Bolt's method. The diagnostic performance of this algorithm is particularly enhanced in patients with ventricular dilatation. The semi-quantitative evaluation technique based on standardized uptake value (SUV), that is, the dopamine transporter standardized uptake value (DaTSUV), was also developed [3]. However, DaTSUV (cut-off=6.8) was not as efficient as the SBR (cut-off=4.32) for dif-

ferentiating dNDD from non-dNDD. On the other hand, the putamen-to-caudate ratio was shown to be a useful measure to differentiate patients with early PS from control subjects [4]. This indicates that assessing the distribution of tracer uptake, and not just its ratio to the background, such as SBR, may be able to detect small changes occurring in the early stage of disease. However, as the resolution of single photon emission computed tomography (SPECT) is very limited, it is difficult to accurately delineate the border between the caudate and putamen, which would also affect the quantification. From these viewpoints, we thought that texture analysis, which directly evaluates the distribution and heterogeneity of tracer uptake, would be useful to capture the states of diseases, such as PS, PD, and DLB manifesting in the form of uneven loss of tracer uptake within the striatum. Texture analysis provides information about the heterogeneity of tracer uptake noninvasively from routine images. The first-order texture features based on the gray-level histogram method (GLHM) and second-order texture features calculated using the spatial gray level dependence method (SGLDM) are the most widely used texture features. The first-order texture features describe the global gray-level intensity distribution inside the structure, which provides an overall view of the data. On the other hand, the SGLDM features describe the spatial relationships of pairs of pixels or voxels with specific grey-level intensities, in certain directions and with certain distances between them [5]. In recent years, texture analysis has been widely used as a technique to analyze the characteristics and distribution of gray levels within pixels or voxels in medical images, enabling the evaluation of heterogeneity of tracer distribution and the clarification of the details of microstructures that are usually unrecognizable or indistinguishable to the human eye [6]. Texture analysis is thought to enable improvements in experience-dependent and subjective diagnoses of diseases by radiologists, by providing a large amount of objective information of the lesion, thereby assisting them in making a more accurate diagnosis.

In this study, we selected first-order features based on GLHM, that is, mean, variance, skewness, and kurtosis, that are more reproducible than some other texture features to assess the distribution of ^{123}I-FP-CIT within the striatum, for the differentiation between AD and DLB subtypes.

Materials and Methods

Patients

This study included a total of 122 subjects, with probable DLB (n=35), possible DLB (n=23), AD (n=44), and normal controls (n=20), who underwent SPECT/computed tomography (CT) using ^{123}I-FP-CIT (DaTSCAN, Nihon Medi-physics, Tokyo, Japan). The patients were clinically diagnosed by geriatric medicine specialists according to the clinical diagnostic criteria of DLB [7], and guidelines for the diagnosis of Alzheimer's disease by the National Institute on Aging and Alzheimer's Association [8]. Patients who had dementia induced by drugs and cerebrovascular diseases were excluded.

The data analyzed in this study was obtained in a previous study, which was a prospective study conducted in 2014 by Shimizu et al. [9]. This previous study was approved by the Ethics Committee of Tokyo Medical University Hospital. Informed consent was obtained from all subjects (either the subjects themselves or their closest relative) before entry, following a detailed explanation of the study's aim. In accordance with the research plan, the fees of ^{123}I-FP-CIT examination of the patients with AD and normal controls were paid for using the research funds of the Department of Geriatric Medicine of Tokyo Medical University Hospital. All procedures were performed in accordance with the ethical standards on human investigation and with the principles of the Declaration of Helsinki. In this study, we retrospective analyzed these subjects with the approval of the Ethics Committee of our Tokyo Medical University Hospital (study approval no.:T2019-0037).

Image acquisition

All SPECT images were scanned 3 to 4h after a bolus intravenous injection of 167MBq of ^{123}I-FP-CIT using a dual-headed gamma camera (Siemens Symbia 16T, Germany) fitted with low-medial energy parallel hole collimators, and with a 20% energy window set at approximately 159KeV. Images were acquired for 210 sec over a 360° orbit × 8 rotations on a 128×128 matrix, with a pixel size of 4.4mm, slice thickness of 4.4mm, and a zoom of 1.4. The overall image acquisition time was 28min.

A CT scan was performed after the SPECT scan, using the same SPECT/CT equipment. The following scanning parameters were kept constant during the helical scanning mode: 1.0s gantry rotation time, 130kVp, 220mAs, helical pitch: 0.7, and slice width: 1.0mm. Images were reconstructed at 2.0mm thickness using the Flash 3D algorism (Siemens Healthineers), with 8 iterations in 6 subsets, followed by attenuation correction by CT.

Texture analysis

A summated SPECT image of 7 to 10 (9.3±1.2) slices, which included the bilateral striatum reconstructed at 4.4-mm intervals with a 4.4-mm thickness, was made by the multipurpose image analysis software DRIP (Daemon Research Image Processor version 3.0.2.0; FUJIFILM RI Pharma Ltd., Tokyo, Japan). On these 3D-^{123}I-FP-CIT images, a rectangular region of interest (ROI) including the bilateral striatum was set and analyzed (ROI method) (Figure 1). In this method, the background signal, and tracer accumulation in the cerebrum, except for that in the bilateral striatum was masked, and was not included in the analysis.

Texture analysis was performed using the image processing software Pop Imaging Ver.6.10 (Digital being kids, Ltd., Yokohama, Japan). The GLHM analyzes the mean (1), variance (2), skewness (3), and kurtosis (4) using the formulas shown below.

$$\mu = \sum_{i=0}^{n-1} i \cdot p(i) \qquad (1)$$

$$P^2 = \sum_{i=0}^{n-1} (1-\mu)^2 \cdot p(i) \qquad (2)$$

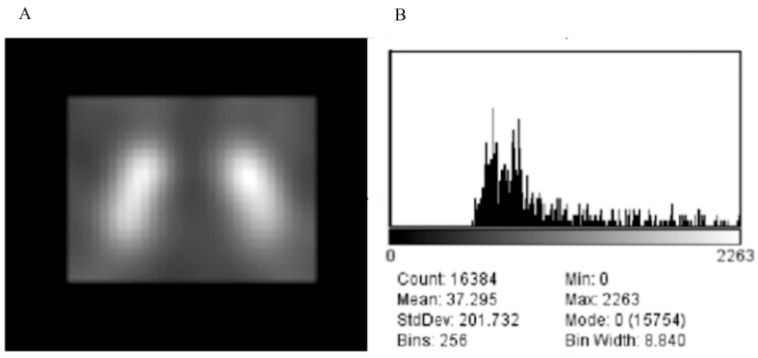

Figure 1. ROI method. A) A rectangular ROI set on the bilateral striatum. B) Texture analysis based on the GLHM.

$$s = \frac{\sum_{i=0}^{n-1}(1-\mu)3 \cdot p(i)}{p3} \quad (3)$$

$$k = \frac{\sum_{i=0}^{n-1}(1-\mu)4 \cdot p(i)}{p4} \quad (4)$$

The density histogram P(i), which is the total area under the probability distribution curve, was normalized to 1. For comparison, we used the SBR method as a conventional assessment.

Statistical analysis

To compare the parameters between patients with probable DLB, possible DLB, and AD, and normal controls, the Kruskal-Wallis test and Mann-Whitney U test with Bonferroni correction were used. P-values of less than 0.05 were considered to indicate statistically significant differences between 2 groups. ROC analysis was performed and the area under the curve (AUC) was calculated to determine optimal cutoff values of each factor. Furthermore, discriminant analysis was performed to predict the probability of belonging to each group. All data were analyzed by R software.

Results

Patient characteristics are shown in Table 1. The results of ROI method and SBR method analysis of the 4 groups are shown in Table 2. Box-and-whisker plots of skewness and kurtosis are shown in Figure 2. Regarding intergroup comparisons of each group by the Kruskal-Wallis test and Mann-Whitney U test with Bonferroni correction, the differentiation of AD and DLB was possible using every parameter by both the ROI method and the SBR method. Possible DLB and probable DLB could be differentiated only by skewness and kurtosis (Table 3). ROC analyses were used to set the cut-off texture features for differentiating probable DLB from possible DLB, AD, and normal controls (Figure 3). Among them, skewness showed the highest AUC with a value of 0.927 (P<0.05; 95% confidence interval [CI]: 0.882-0.972), sensitivity of 97.1%, specificity of 77.0%, using the cut-off point of 6.8. Regarding kurtosis, the AUC was 0.925 (P<0.05; 95% [CI]: 0.879-0.970, sensitivity was 97.1%, and specificity was 81.6%, with the cut-off point of 53.4. Figure 4 shows ROC analysis to set the cut-off texture features for differentiating probable DLB and possible DLB from AD and normal controls. Among them, kurtosis showed the highest AUC, with a value of 0.919 (P<0.05; 95% [CI]: 0.869-0.969), sensitivity of 79.3%, and specificity of 93.8%, using the cut-off point of 53.4. As for skewness, the AUC was 0.903 (P< 0.05, 95% [CI]: 0.847-0.958), sensitivity was 65.5%, and specificity was 98.4%, using the cut-off point of 6.4. Figure 5 and Table 4 show a scatter plot using the first 2 discriminant functions by the ROI method. When function 1 is a positive value, the patient is likely to have AD or to not have dementia (normal), and when it is negative, the patient is likely to have DLB. When the value of function 2 is positive, probable DLB or AD is likely, but if it is negative, determination is difficult.

Discussion

In a previous study by Shimizu et al. (2016), the diagnostic value of ^{123}I-FP-CIT and iodine-123-metaiodobenzylguanidine (^{123}I-MIBG) were compared in their ability to differentiate DLB from AD. Mean SBR on ^{123}I-FP-CIT were markedly lower in patients with DLB than in those with AD (5.2±1.0 vs 2.7±1.3; cut-off: 4.18; P<0.0001) [9]. However, some patients with DLB had SBR within the normal range but showed decreased ^{123}I-MIBG uptake. Moreover, there was a significantly higher frequency of patients with parkinsonism in the abnormal ^{123}I-FP-CIT group than in the normal ^{123}I-FP-CIT group. On the other hand, there was a higher frequency of patients with rapid eye movement sleep behavior disorder (RBD) in the abnormal ^{123}I-MIBG uptake group than in the normal ^{123}I-MIBG uptake group [9]. These results suggested that semi-quantification of SBR alone is not sufficient, and combined assessment of these scintigraphic methods is useful to differentiate DLB from AD.

There are some reports on the association between spe-

Table 1. *Patient characteristics.*

	Prob DLB	Pos DLB	AD	Normal
Number of patients	35	23	44	20
Age	80±5	81±5	82±7	80±7
Sex (men/women)	17/18	11/12	11/33	7/13
MMSE score	21.7±5.2	23.9±4.6	22.5±5.4	
Hoehn & Yahr score	2.6±1.0	2.3±1.0		
Parkinsonism, n (%)	32 (91%)	21 (91%)		
Hallucination, n (%)	26 (74%)	2 (9%)		
RBD, n (%)	21 (60%)	3 (13%)		

Pro DLB: Probable dementia with Lewy bodies; Pos DLB: Possible dementia with Lewy bodies; AD: Alzheimer disease; MMSE: Mini-Mental State Examination; RBD: Rapid eye movement sleep behavior disorder

Table 2. *Comparison of parameters obtained by the ROI method and the SBR method.*

	Prob DLB	Pos DLB	AD	Normal
Mean	35.1±7.9	36.0±11.2	43.9±6.5	42.8±6.9
Variance	3,7901.1 ± 1,5045.4	50,203.9 ± 31,251.8	68,488.0 ± 20,995.1	70593.2±21792.7
Skewness	5.9±0.5	6.7±0.8	7.4±0.5	7.5±0.6
Kurtosis	41.0±8.2	52.0±13.4	67.3±9.5	68.7±11.4
SBR method				
	Prob DLB	**Pos DLB**	**AD**	**Normal**
SBR	2.3±1.1	2.6±1.3	5.2±1.0	5.8±1.4

ROI: Region of interest; SBR: Specific binding ratio by Livia Tossici-Bolt's method

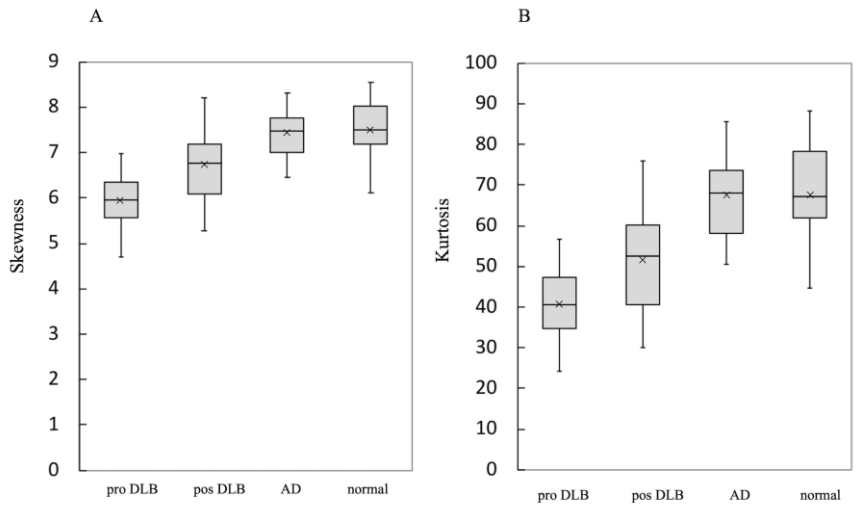

Figure 2. Box-and-whisker plots of skewness and kurtosis.

Table 3. Intergroup comparisons by the ROI method and the SBR method.

ROI method		
Group A	**Group B**	**P-value**
Mean		
Pro DLB	Pos DLB	1.000
Pro DLB	AD	4.50E-06**
Pro DLB	Normal control	0.002**
Pos DLB	AD	0.0032**
Pos DLB	Normal control	0.0404*
AD	Normal control	1.000
Variance		
Pro DLB	Pos DLB	1.000
Pro DLB	AD	8.10E-09**
Pro DLB	Normal control	2.80E-07**
Pos DLB	AD	0.0022**
Pos DLB	Normal control	0.0078**
AD	Normal control	1.000
Skewness		
Pro DLB	Pos DLB	0.01332*
Pro DLB	AD	3.50E-12**
Pro DLB	Normal control	6.70E-10**
Pos DLB	AD	0.00032**
Pos DLB	Normal control	0.00086**
AD	Normal control	1.000
Kurtosis		
Pro DLB	Pos DLB	0.02868*
Pro DLB	AD	1.80E-12**
Pro DLB	Normal control	1.30E-09**
Pos DLB	AD	5.90E-05**
Pos DLB	Normal control	0.00047**
AD	Normal control	1.000
SBR method		
Group A	Group B	P-value
SBR		
Pro DLB	Pos DLB	1
Pro DLB	AD	5.80E-12**
Pro DLB	Normal control	2.70E-08**
pos DLB	AD	2.40E-08**
pos DLB	Normal control	2.40E-08**
AD	Normal control	0.29

**P<0.05, **P<0.01 by Mann–Whitney U test*

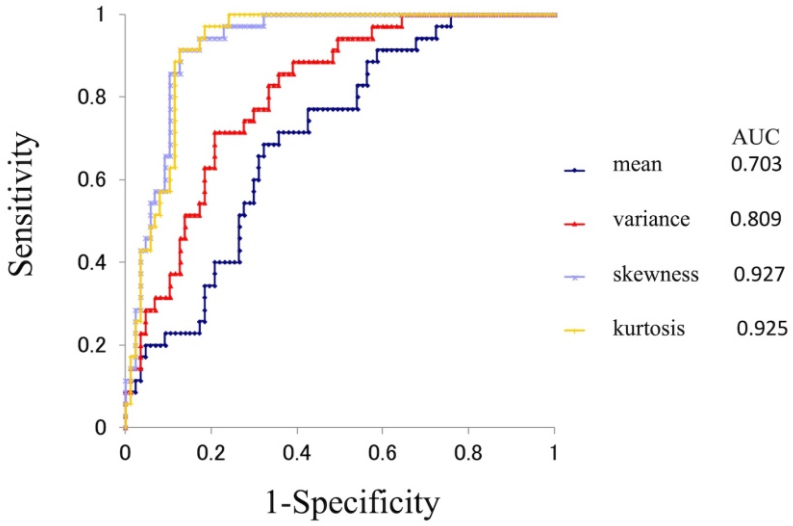

Figure 3. ROC analysis to differentiate probable DLB from possible DLB, AD, and normal controls.

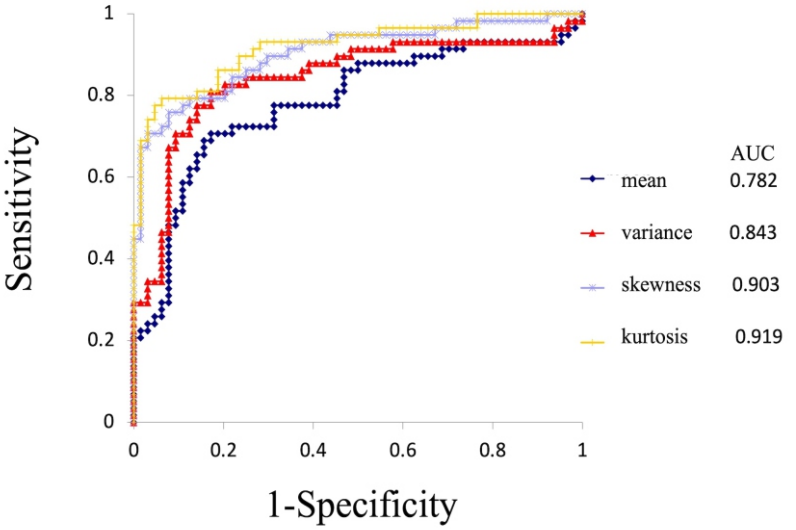

Figure 4. ROC analysis to differentiate probable DLB and possible DLB from AD and normal controls.

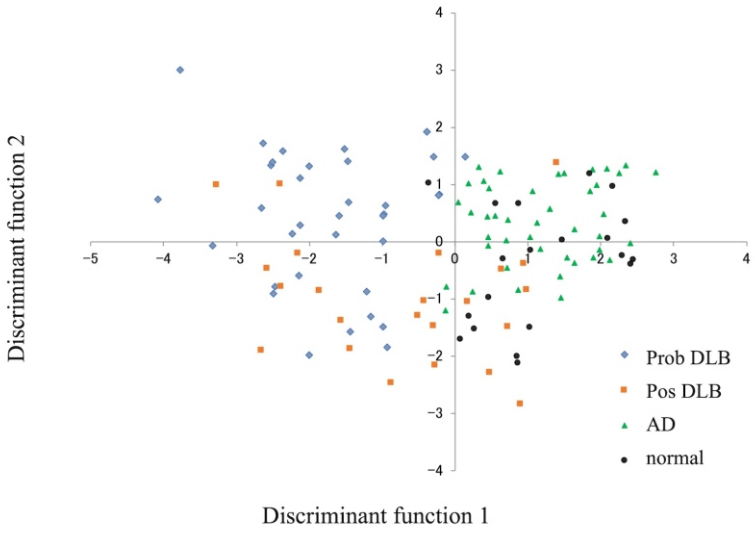

Figure 5. Scatter plot of discriminant analysis performed by the ROI method.

Table 4. *Discriminant analysis by the ROI method.*

Function coefficients		
	Function 1	**Function 2**
Mean	0.1617	0.1149
Variance	0.0000	0.0000
Skewness	1.5802	7.9106
Kurtosis	0.0162	0.4478
Constant	15.8845	26.6818

Results of the discriminant analysis by groups

	Predicted group			
	Prob DLB	**Pos DLB**	**AD**	**Normal**
Actual group	**n (%)**	**n (%)**	**n (%)**	**n (%)**
Prob DLB (n=35)	**26 (74.3)**	6 (17.1)	3 (8.6)	0
Pos DLB (n=23)	5 (21.7)	**13 (56.5)**	1 (4.3)	4 (17.4)
AD (n=44)	0	3 (6.8)	**30 (68.2)**	11 (25.0)
Normal (n=20)	1 (5.0)	3 (15.0)	6 (30.0)	**10 (50.0)**

Total of the actual group correctly classified: 79 (64.8)

cific neurological symptoms and the dysfunction of specific sites in the striatum. For example, it is known that different subregions within the putamen and caudate are associated with various clinical symptoms of parkinsonism [10]. Furthermore, Kasanuki reported that among the Lewy body disease-associated nonmotor symptoms, the duration of olfactory dysfunction and RBD demonstrated a negative correlation with SBR scores in prodromal DLB [11]. Nonmotor symptoms, such as RBD, are also likely to cause the uneven loss of tracer uptake within the striatum, although the interpretation is not simple.

Dementia with Lewy bodies is diagnosed mainly by a combination of core clinical features (fluctuating cognition, recurrent visual hallucination, RBD, and parkinsonism), and indicator biomarkers (^{123}I-FP-CIT, ^{123}I-MIBG, and EEG) [7]. The progression of disease from possible to probable DLB may be associated with not only the quantitative exacerbation of symptoms but also the appearance of other clinical symptoms. In fact, between the probable DLB group and possible DLB group in this study, there was no significant difference in Mini-Mental State Examination (MMSE), Hoehn & Yahr scores, and SBR, but large differences were observed in the frequency of hallucinations and RBD (Table 1). Therefore, the prediction of disease prognosis by texture analysis appears effective.

In this study, we hypothesized that not only motor symptoms, but also non-motor symptoms were reflected as an uneven loss of ^{123}I-FP-CIT uptake in the striatum, and possible DLB, probable DLB, and AD could be differentiated by the texture feature of the striatum. As a result, skewness and kurtosis within a specific ROI analyzed by the GLHM were shown to be a relevant measure to differentiate DLB from AD, and probable DLB from possible DLB. It was not possible to identify which part of the striatum reflected each symptom, but we demonstrated that an uneven distribution reflects various symptoms. To our knowledge, this is the first report demonstrating that texture analysis of ^{123}I-FP-CIT imaging is useful for the differentiation between AD and DLB subtypes although there are several approaches for the diagnosis of PS [12, 13].

There are some difficulties in the evaluation using texture analysis. For example, many statistical calculations are required, and which calculations are used depends on the researcher, as no consensus has been reached. In this study, a high diagnostic value was obtained by GHLM analysis, which is the simplest analysis method, and hence can be easily retested at any facility [14]. Rahmin (2016) reported that a number of Haralick textural features that are considered to characterize the uptake of ^{123}I-FP-CIT were found to significantly correlate with the clinical measures of Unified Parkinson's Disease Rating Scale (UPDRS) and disease duration of PD [8]. This image analysis method included registration of SPECT images onto the corresponding magnetic resonance imaging (MRI) images, and automatic ROI extraction on the MRI images. In this study, we did not harmonize or register the SPECT images onto the MRI images, because the proce-

dure was difficult and arbitrary, as ^{123}I-FP-CIT shows almost no accumulation other than in the striatum. Therefore, we simply set the ROI to include the striatum, and performed the analyses.

This study had the following limitations. First, the diagnosis of DLB, AD, and normal controls was clinically, rather than pathologically based, and hence only patients with definite and obvious disease were analyzed. In the future, it will be important to analyze more patients without a definitive diagnosis, and patients with combined AD and DLB. Second, making a rectangular ROI to surround the bilateral striatum was sometimes not reproducible, particularly when the accumulation of ^{123}I-FP-CIT in the striatum was low. For this reason, we think a non-ROI method would be simpler and superior to an ROI method. Therefore, if similar results can be obtained, we believe the non-ROI method is more favorable. However, we found no advantages in the results of the non-ROI method over the ROI method, probably because when the entire brain including the cortex is analyzed, the features of ^{123}I-FP-CIT distribution in the striatum cannot be captured sufficiently (data not shown). However, the analytical value was not affected by the individual ROIs unless cortical accumulation was included in the ROI (data not shown). Furthermore, needless to say, comparing statistical texture features across different SPECT devices or even across differing reconstruction algorithms is expected to be unsuccessful. Therefore, unifying data acquisition protocols and standardizing analysis methods may be the key to the routine clinical use of texture feature analysis in the future.

In conclusion, in the assessment of the efficacy of ^{123}I-FP-CIT for differentiating DLB and AD, the mean, variance, skewness, and kurtosis by GLHM using the ROI method was found to be as useful as the SBR method. Moreover, possible DLB and probable DLB could be differentiated by skewness and kurtosis. Our results demonstrated the ability to obtain valuable information using texture analysis, beyond conventional quantitative methods. Textural features may hence have considerable potential as biomarkers for the assessment of dementia. Further longitudinal studies are needed to substantiate these findings in the future.

Acknowledgements

We thank N. Miyajima, T. Aida, and D. Hakamata of the Department of Nuclear Medicine of Tokyo Medical University for their support and technical assistance. We are also grateful to Helena Akiko Popiel of the Department of International Medical Communications of Tokyo Medical University for reviewing the manuscript.

The authors declare that they have no conflicts of interest.

Bibliography

1. Tossici-Bolt L, Hoffmann SM, Kemp PM et al. Quantification of ^{123}I-FP-CIT SPECT brain images: an accurate technique for measurement of the specific binding ratio. *Eur J Nucl Med Mol Imaging* 2006; 33: 1491-9.
2. Iwabuchi Y, Nakahara T, Kameyama M et al. Impact of the cerebrospinal fluid-mask algorithm on the diagnostic performance of ^{123}I-Ioflupane SPECT: an investigation of parkinsonian syndromes. *EJNMMI Res* 2019; 9: 85.
3. Wakabayashi Y, Takahashi R, Kanda T et al. Semi-quantitative dopamine transporter standardized uptake value in comparison with conventional specific binding ratio in ^{123}I FP-CIT single-photon emission computed tomography (DaTscan). *Neurol Sci* 2018; 39: 1401-7.
4. Matesan M, Gaddikeri S, Longfellow K et al. I-123 DaTscan SPECT Brain Imaging in Parkinsonian Syndromes: Utility of the Putamen-to-Caudate Ratio. *J Neuroimaging* 2018; 28: 629-34.
5. Mayerhoefer ME, Materka A, Langs G et al. Introduction to Radiomics. *J Nucl Med* 2020; 61: 488-95.
6. Castellano G, Bonilha L, Li LM, Cendes F. Texture analysis of medical images. *Clin Radiol* 2004; 59: 1061-9.
7. McKeith IG, Boeve BF, Dickson DW et al. Diagnosis and management of dementia with Lewy bodies: Fourth consensus report of the DLB Consortium. *Neurology* 2017; 89: 88-100.
8. McKhann GM, Knopman DS, Chertkow H et al. The diagnosis of dementia due to Alzheimer's disease: recommendations from the National Institute on Aging-Alzheimer's Association workgroups on diagnostic guidelines for Alzheimer's disease. *Alzheimers Dement* 2011; 7: 263-9.
9. Shimizu S, Hirao K, Kanetaka H et al. Utility of the combination of DAT SPECT and MIBG myocardial scintigraphy in differentiating dementia with Lewy bodies from Alzheimer's disease. *Eur J Nucl Med Mol Imaging* 2016; 43:184-92.
10. Rahmim A, Salimpour Y, Jain S et al. Application of texture analysis to DAT SPECT imaging: Relationship to clinical assessments. *Neuroimage Clin* 2016; 12: e1-e9.
11. Kasanuki K, Iseki E, Ota K et al. ^{123}I-FP-CIT SPECT findings and its clinical relevance in prodromal dementia with Lewy bodies. *Eur J Nucl Med Mol Imaging* 2017; 44: 358-65.
12. Morbelli S, Arnaldi D, Cella E et al. Striatal dopamine transporter SPECT quantification: head-to-head comparison between two three-dimensional automatic tools. *EJNMMI Res* 2020; 10: 137.
13. Rahmim A, Huang P, Shenkov N et al. Improved prediction of outcome in Parkinson's disease using radiomics analysis of longitudinal DAT SPECT images. *Neuroimage Clin* 2017; 16: 539-44.
14. Miles KA, Ganeshan B, Hayball MP. CT texture analysis using the filtration-histogram method: what do the measurements mean? *Cancer Imaging* 2013; 13: 400-6.